2-Hz 109-nm mirrorless laser

M. H. Sher, S. J. Benerofe, J. F. Young, and S. E. Harris

Edward L. Ginzton Laboratory, Stanford University, Stanford, California 94305

Received July 28, 1989; accepted June 8, 1990

We report 2-Hz operation of a single-pass 109-nm laser with a small-signal gain of exp 33 and a saturated output energy of 1 μJ. The laser is based on an oblique-incidence, laser-produced-plasma pumping geometry and requires only 500 mJ of 1064-nm energy in a 0.5-nsec pump pulse. We use the laser to produce a two-slit interference pattern and demonstrate a focusable intensity of greater than 10^9 W/cm^2.

We extended our oblique-incidence traveling-wave laser-produced-plasma pumping geometry[1] to 82.5° from normal (see Fig. 1). Using only 500 mJ of 1064-nm pump energy in a 0.5-nsec pulse, we observed a total small-signal gain of exp 33 and a saturated output energy of 1 μJ on the Xe III 109-nm Auger-laser transition.[2] Previous experiments on the Xe laser required significantly more pump energy to produce similar or smaller gains and were limited to extremely low repetition rates.[1–3] The present energy requirement makes it possible to run the 109-nm laser at the relatively high repetition rate of 2 Hz.

As was discussed in Ref. 1, the oblique-incidence grooved-target geometry has several advantages for efficient pumping of photoionization lasers. It produces a nearly synchronous, traveling-wave excitation source of a length that is determined by the angle of incidence. The grooved target brings the local angle of incidence of the beam-intercepting surfaces back to near normal, minimizing reflection and reducing the total length of the plasma. As a result, the pump-laser intensity on the target is independent of the angle of incidence, and the laser's efficiency of conversion to soft x rays is nominally independent of length.

The advantages of distributing the soft-x-ray source over an extended length can be understood qualitatively by using a simple model. The gain of the Xe laser, as well as of other photoionization lasers, is reduced by a high density of free electrons that are created in the pumping process. Thus, for a given Xe density and pump-pulse length, there is an optimum soft-x-ray flux that will result in a maximum gain coefficient. Because the soft-x-ray flux from a laser-produced plasma diverges, this gain coefficient will occur at some finite distance y above the surface of the target. If this distance is large compared with the groove spacing, the spatial variation of the flux from the series of small plasmas will be similar to that of a line source. As the angle of incidence is increased and the soft-x-ray energy is distributed over a longer length L, the maximum gain coefficient should remain constant as the region of optimum flux simply moves closer to the target as $1/L$. The total gain–length product will then be proportional to L. In addition, since both transverse dimensions of the maximum gain region will be proportional to y, and the laser output should be dominated by emission from this volume, a small increase in the length of the laser will produce a large improvement in the quality of the output beam. The laser-emission solid angle should scale as $1/L^4$, the Fresnel number as $1/L^3$, and the energy stored in the volume of maximum gain as $1/L$. One should therefore pump a photoionization laser at the maximum practical angle of incidence.

There are limits to this reasoning. The model breaks down if the pump energy per unit length is reduced to the point where y is of the order of the groove spacing or the transverse spot size. At this distance from the target the flux will no longer be constant in the longitudinal direction, and the line-source analogy will fail. Another restriction arises if the smallest dimension of the individual plasma spots, which is determined by both the angle of incidence and the groove spacing, becomes small enough to reduce the absorption of the pump laser and the soft-x-ray conversion efficiency.[4]

In order to test the predicted scaling of the gain–length product in Xe lasers, we compared the small-signal gain and large-signal behaviors that were produced at two different angles of incidence. A 2.1 cm × 1.0 cm elliptical 1064-nm laser beam (the smaller transverse dimension reduced the effect of aberrations in the tilted lenses and improved the focus) was used at $\theta = 67°$ and at $\theta = 82.5°$ to pump 5.3- and 16-cm-long lasers. The ratio of lengths and hence the predicted improvement in the gain–length product of the lasers was a factor of 3. The pump beam, which delivered 500 mJ of energy to the target in a 0.5-nsec pulse, was produced by a Nd:YAG laser system that was running at a repetition rate of 2 Hz. The cylindrical lenses for the 67° and 82.5° geometries had normal incidence focal lengths of 65 and 115 cm, respectively; the lens that was used at 82.5° had a specially developed antireflection coating[5] that transmitted 85% of the p-polarized light. The target was a stainless-steel tube, threaded at 31.5 grooves/cm, and the ambient Xe pressure was 10 Torr. We were able to hold several important pumping parameters constant by compensating for the slightly higher transmission of the lens used at 67° and by changing the groove angle of the target, α, from 45° to 60°. For both configurations the local angle of incidence $(\theta - \alpha)$ was 22°, the transverse spot size was 150 μm, and the intensity on target was 5×10^{10} W/cm^2. The longitudinal dimension of the individual plasmas, however, could not be held constant without changing the groove spacing.

0740-3224/91/010114-03$05.00

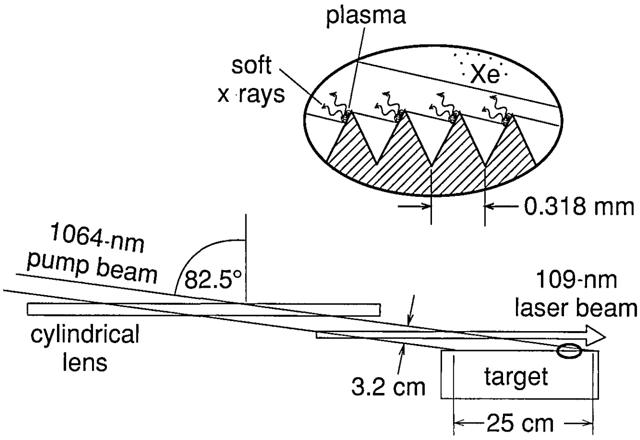

Fig. 1. Schematic of 25-cm-long laser produced by 3.2-cm beam in 82.5° pumping geometry.

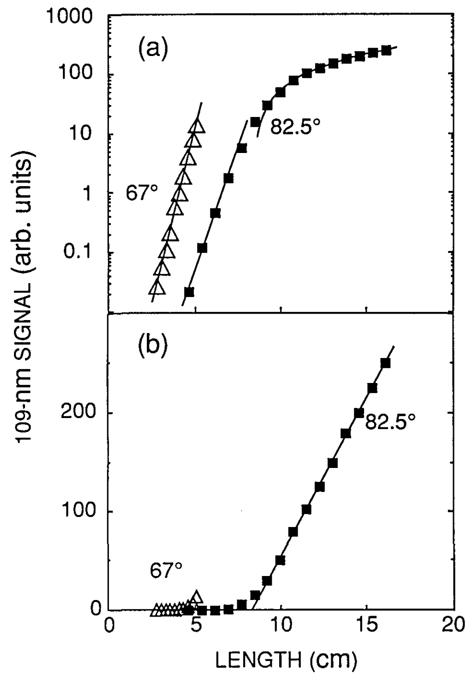

Fig. 2. Comparison of lasers produced by 2.1-cm beam used at 67° and at 82.5° incidence. Signal versus length curves are shown on (a) semilogarithm and (b) linear scales.

For the 67° geometry the plasmas were 135 μm long, whereas at 82.5° they were only 45 μm long. A 350-μm-diameter aperture placed 1 cm from the end of the plasma was used to define the observed volume, and the 109-nm signal was detected with a time-integrating multichannel plate electron multiplier (response time of 700 psec) that was mounted on a 0.2-m vacuum spectrometer.

The result of the angle comparison is shown in Fig. 2. While the 67° geometry produced a gain coefficient of 2.8 cm^{-1} over 5.3 cm, the 82.5° geometry produced a gain coefficient of 1.9 cm^{-1} over 16 cm. The ratio of the gain–length products is 2. The discrepancy with the factor of 3 that is predicted by simple scaling may have arisen from the 82.5° laser's running at a distance from the target (300–400 μm as determined from the optimum aperture position) that was comparable with the groove spacing. Although the observed change in the gain–length product does not quantitatively agree with the simple model, the increase in the angle of incidence of the pump beam improved the gain sufficiently to saturate the lasing transition fully and produced an increase by a factor of 20 in the 109-nm signal.

After verifying the advantage of distributing a fixed amount of pump flux over an extended length, we expanded the pump beam to 3.2 cm and used the 82.5° geometry to produce the 25-cm-long laser shown in Fig. 1. The intensity on target was only 3×10^{10} W/cm^2, and the ambient Xe pressure was increased to 15 Torr. At this angle of incidence the leading edge of the plasma moves along the target at an effective speed of 1.009 times the speed of light, so the traveling-wave mismatch over the 25 cm was only 7 psec. Figure 3 is a graph of the 109-nm signal versus length from a section-by-section small-signal gain measurement. It shows fairly uniform pumping of the central 18 cm of the target, where the gain coefficient averages 1.6 cm^{-1}, with significant reduction of the gain at the two ends. The total gain–length product is 33. The large-signal behavior of the laser was quite similar to that shown for the 82.5° geometry in Fig. 2, with the length scale multiplied by a factor of 3/2. The energy in the full-length output was 1 μJ (measured by using a vacuum photodiode with an Al photocathode), which corresponds to an efficiency of 2×10^{-6}.

A Kentech soft-x-ray streak camera equipped with a 10 nm-thick Au photocathode deposited onto a 1-mm-thick LiF substrate was located 53 cm from the laser and was used to take both time-resolved and time-integrated beam profiles. Without the aperture the laser produced an approximately 4 mm × 6 mm teardrop-shaped spot with the axis of symmetry perpendicular to the target. This profile was time resolved with the streak-camera slit oriented both perpendicular and tangent to the target. Taken together, the streaks suggest that the beam originates in a narrow volume along the target but then diverges to form a semicircular pattern with reduced emission in the central region. The simplest explanation for this behavior, an explanation supported by the absence of the behavior for shorter, unsaturated lengths, is spatial gain depletion. The whole event lasts ~250 psec.

When the 350-μm aperture that was used in the gain measurements was positioned for maximum throughput (~15%) the spot produced on the streak camera was 1 mm in diameter and quite symmetric, indicating a beam diver-

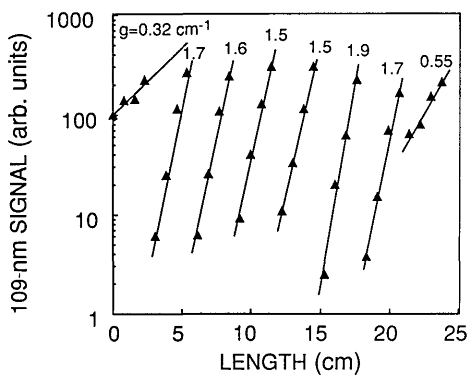

Fig. 3. Sectional signal versus length curves of 25-cm-long laser. The average gain coefficient of the central 18 cm is 1.6 cm^{-1}, and the total small-signal gain is exp 33.

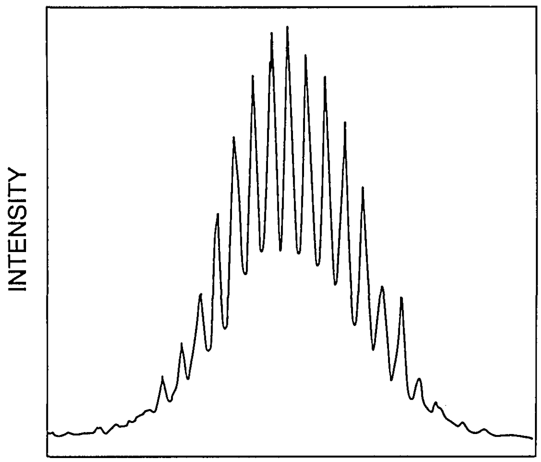

Fig. 4. Double-slit interference fringes. See text for an explanation.

gence of 0.6 mrad. The temporal profile of this beam was 40 psec FWHM, with significant saturation steepening of the rising edge. We focused the apertured beam by using a SiO_2 mirror with a focal length of 14 cm, placed 2 m from the laser at 3° off normal incidence. Our measured 75% energy transmission through a 10-μm-diameter pinhole is consistent with a Gaussian focal spot of $w_0 = 6\ \mu$m. Using a commercially available 50% reflective coating, one could obtain a focused intensity of greater than 10^9 W/cm^2.

In a first step toward applying this type of laser to coherent imaging, we have generated a double-slit interference pattern. We placed a double air slit (two 10-μm slits, 100 μm apart) 66 cm from the apertured laser and placed the streak camera 58 cm from the slits. An intensity plot of a single-shot interference pattern is shown in Fig. 4. The limited fringe visibility is consistent with that expected from an incoherent source of the same diameter as the aperture. The temporal coherence of the laser was not measured.

Two significant practical problems involved in extending this geometry to these (and perhaps even more oblique) angles of incidence arise because of the choice of focusing optic. A cylindrical lens used at this angle introduces aberrations in the focus and requires a specially designed, wavelength- and polarization-specific, antireflection coating. One possible solution to these problems would be the use of a cylindrical mirror as the focusing optic.

In this study we demonstrated the advantage and discussed some of the limitations of the oblique-incidence, grooved-target geometry for pumping photoionization lasers. The result is, to our knowledge, the first high-repetition-rate, short-wavelength, photoionization laser. We briefly characterized the laser and used its 2-Hz repetition rate to make coherence and focusing measurements.

ACKNOWLEDGMENTS

The authors thank J. J. Macklin for helpful discussions and S. Jeng for his enthusiasm in the development of the 82.5° antireflection coating. M. H. Sher acknowledges the assistance of an AT&T Ph. D. Scholarship. This work was jointly supported by the U.S. Office of Naval Research, the U.S. Air Force Office of Scientific Research, the U.S. Army Research Office, and the Strategic Defense Initiative Organization.

REFERENCES

1. M. H. Sher, J. J. Macklin, J. F. Young, and S. E. Harris, "Saturation of the Xe III 109-nm laser using traveling-wave laser-produced-plasma excitation," Opt. Lett. **12,** 891 (1987).
2. H. C. Kapteyn, R. W. Lee, and R. W. Falcone, "Observation of a short-wavelength laser pumped by Auger decay," Phys. Rev. Lett. **57,** 2939 (1986).
3. Guang-Yu Yin, C. P. J. Barty, D. A. King, D. J. Walker, S. E. Harris, and J. F. Young, "Low-energy pumping of a 108.9-nm xenon Auger laser," Opt. Lett. **12,** 331 (1987).
4. C. E. Max, "Physics of the coronal plasma in laser fusion targets," in *Laser Plasma Interactions,* R. Balian and J. C. Adams, eds. (North-Holland, Amsterdam, 1982).
5. Coating developed by S. Jeng of J. L. Wood Optical Systems, Santa Ana, Calif.